# Operator-based linearization approach for modeling of multiphase multi-component flow in porous media

Voskov, Denis V.

**DOI**
10.1016/j.jcp.2017.02.041

**Publication date**
2017

**Document Version**
Accepted author manuscript

**Published in**
Journal of Computational Physics

**Citation (APA)**
Voskov, D. V. (2017). Operator-based linearization approach for modeling of multiphase multi-component flow in porous media. *Journal of Computational Physics*, *337*, 275-288. https://doi.org/10.1016/j.jcp.2017.02.041

Postprint of Journal of Computational Physics
Volume 337, 15 May 2017, Pages 275–288
Link to formal publication (Elsevier): http://dx.doi.org/10.1016/j.jcp.2017.02.041

# Operator-based linearization approach for modeling of multiphase multi-component flow in porous media

Denis V. Voskov

*Delft University of Technology*
*Department of Geoscience & Engineering*
*Stevinweg 1, 2628 CN Delft, NL*
*d.v.dvoskov@tudelft.nl*

---

## Introduction

Reservoir simulation of complex physical processes requires on the solution of the nonlinear model equations. These include partial differential equations describing the conservation of mass, momentum, and energy as well as different types of local constraints that define phase behavior and/or chemical reactions in the system. A general purpose process of robustly solving these equations typically includes highly implicit (fully or adaptively) approximation in time to avoid numerical limitations (such as a CFL limit for a multi-component transport) and complex flux approximations to preserve the accuracy in spatial discretization. Both of these approximations introduce nonlinearity into the system of equations.

In reservoir simulation, different formulations are used for solving the system of governing equations. These formulations usually differ in types of nonlinear unknowns used for the solution, see [1] for an extensive overview. For the purpose of classification, all nonlinear formulations can be separated into two classes: mass-based and phase-based formulations. The mass-based formulation [2, 3] uses mass-related variables (overall composition or molar mass) for solving a nonlinear system of equations. In the phase-based (also called natural) formulation [4], variables related to a phase (saturation and phase fractions) serve as nonlinear unknowns.

Recently, several advanced nonlinear formulations were developed for compositional simulations [5, 6]. All of these approaches propose a better way of dealing with phase changes. However, these formulations were never tested for complex realistic problems. The idea described in [5] was adapted for a general purpose simulation and tested against state of the art approaches [7]. For the problems of practical interest, this formulation demonstrated only insignificant improvements with respect to conventional methods.

After that equations are discretized in space and time, they require a linearization step. Usually, a Newton-based method is used for the linerization implying an assembly of a Jacobian and a residual for the combined system of equations. In general purpose reservoir simulation this is a challenging task. Both value and derivatives of different properties involved in the governing equations need to be computed and stored. This requires fixing nonlinear unknowns and the formulation for the implementation of a simulator code [8, 9]. It is still possible to derive a Jacobian for another formulation on a linear level using a transformation matrix (see [8] for example), but this approach often lacks robustness.

The development of an Automatic Differentiation (AD) technique helps to improve the situation. In several research areas, the utilization of AD makes the solution of the system of nonlinear equations much more flexible. In reservoir simulation, the first attempt to design an AD-based general-purpose simulator was accomplished based on the Automatic Differentiation Expression Template Library (ADETL) developed by Younis [10]. An Automatic Differentiation General Purpose Research Simulator (ADGPRS) was developed using AD-capabilities and the special data-structures of ADETL [11]. This simulator utilizes the idea of having different nonlinear formulations in a single framework providing a consistent platform for the comparison of formulations [7, 12]. ADGPRS creates opportunities for different research directions, including advanced discretization [13], extended physics [14, 15] and inverse capabilities [16].

Using the ADGPRS framework, the new nonlinear strategy called Compositional Space Parametrization (CSP) was developed for compositional simula-

tion [12, 17]. This approach is based on an analysis of compositional displacement in the hyperbolic limit, which indicates that the solution is localized only around the displacement path in tie-line space [18]. In this approach, tie-lines are adaptively parameterized along the displacement solution and the compositional problem is solved using tie-line parameters as nonlinear unknowns. The new tie-line-based approach improves the nonlinear convergence of compositional simulations and the general performance due to a significant reduction in phase equilibrium computations. Recently, the parametrization approach based on sparse grids was suggested for improving the performance of phase behavior [19]. The authors reports significant improvements in CPU time, but their conventional flash algorithm demonstrates a unrealistically high reference time.

While enough attention has been paid to the linearization technique and the solution of the phase behavior problem, the application of the nonlinear solver has also been the object of considerable interest. In the course of the simulation, nonlinear unknowns are updated based on the solution of a linear system. It is a common practice in reservoir simulation to modify the update. Different versions of global or local chopping procedures exist for the nonlinear update. One of the most commonly used in practice is the Appleyard chop [9], where the saturation updates are corrected locally according to the end-points of a relative-permeability function. Another approach is to control unknowns from crossing an inflection point of the fractional flow function [20], which becomes more complex when compositional effects [21], gravity [22], or capillarity with upstream changes [23] are present. All of these methods are trying to resolve the most severe nonlinearities, which are introduced by a combination of properties in the governing equations after the conventional linearization is applied.

In reservoir simulation, we always deal with approximations of discretizations in space and time while resolving all the features of the physical description very accurately. In a lot of cases, this forces the nonlinear solver to struggle and requires advanced methods. In this paper, we present a completely different approach to the linearization of the governing equations that follows the ideas developed by Zaydullin et al. [12]. The discretized version of the conserva-

tion equations is written in an operator form where each term is presented as a product of two operators. The first type of operators depends on the physical properties of the rock and the fluid while the second type depends on the properties altered in space. The first type of operators is parametrized in the physical space of a simulation problem in pre-processing stage. In the course of the simulation, multilinear interpolation is applied for physics-based operators while the second type of operators is evolved conventionally. It is shown that using a limited number of points in the proposed physical representation, the main nonlinearity of a simulation model can be captured quite precisely. The numerical results of an approximation in the linearized space demonstrate better nonlinear convergence with the error in the approximation controlled by the accuracy of the interpolation. In addition, any expensive property evaluations required by the physical model are limited to a few parametrization points, which significantly improves the performance of the simulation. Several additional advantages of the proposed Operator-Based Linearization (OBL) approach are discussed in the last section.

## Modeling approach

In this section, we describe the governing equations and nonlinear formulation for a reservoir simulation problem.

*Conservation equations*

The transport equations for an isothermal system containing $n_c$ components and $n_p$ phases can be written as:

$$\begin{aligned} \frac{\partial}{\partial t}\left(\phi \sum_{j=1}^{n_p} x_{cj}\rho_j s_j\right) &+ \operatorname{div} \sum_{j=1}^{n_p} x_{cj}\rho_j \mathbf{v}_j \\ &+ \sum_{j=1}^{n_p} x_{cj}\rho_j \tilde{q}_j = 0,\ c = 1, \ldots, n_c. \end{aligned} \tag{1}$$

Here, we typically define the coefficients of the equations as functions of spatial coordinate $\boldsymbol{\xi}$ and physical state $\boldsymbol{\omega}$:

- $\phi(\boldsymbol{\xi}, \boldsymbol{\omega})$ – porosity,
- $x_{cj}(\boldsymbol{\omega})$ – the mole fraction of component $c$ in phase $j$,
- $s_j(\boldsymbol{\omega})$ – phase saturations,
- $\rho_j(\boldsymbol{\omega})$ – phase molar density,
- $\mathbf{v}_j(\boldsymbol{\xi}, \boldsymbol{\omega})$ – phase velocity,
- $\tilde{q}_j(\boldsymbol{\xi}, \boldsymbol{\omega})$ – phase rate per unit volume.

To describe the flow of each phase, we use Darcy's law:

$$\mathbf{v}_j \quad = \quad -\Big(\mathbf{K}\frac{k_{rj}}{\mu_j}(\nabla \boldsymbol{p}_j - \gamma_j \nabla \boldsymbol{d})\Big), \; j = 1, \ldots, n_p, \tag{2}$$

where

- $\mathbf{K}(\boldsymbol{\xi})$ – permeability tensor,
- $k_{rj}(\boldsymbol{\omega})$ – relative permeability,
- $\mu_j(\boldsymbol{\omega})$ – phase viscosity,
- $\boldsymbol{p}_j(\boldsymbol{\omega})$ – vector of pressures in phase $j$,
- $\gamma_j(\boldsymbol{\omega})$ – gravity term,
- $\boldsymbol{d}(\boldsymbol{\xi})$ – vector of depths (positive downwards).

By applying a finite-volume discretization on a general unstructured mesh and backward Euler approximation in time, we can transform the conservation equations into

$$\begin{aligned} & V\left((\phi\sum_j x_{cj}\rho_j s_j)^{n+1} - (\phi\sum_j x_{cj}\rho_j s_j)^{n}\right) \\ & -\Delta t\sum_{l\in \boldsymbol{L}}\left(\sum_j x_{cj}^l \rho_j^l T_j^l \Delta\psi^l\right) + \Delta t\sum_j \rho_p x_{cj} q_j = 0. \end{aligned} \tag{3}$$

where $V$ is the volume of a control volume and $q_j = \tilde{q}_j V$ the source of a phase. Here we neglected capillarity, gravity and used a Two-Point Flux Approximation

(TPFA) with upstream weighting introducing the summation over all interfaces $\boldsymbol{L}$ connecting the control volume with another grid blocks. Based on these simplifications, $\Delta\psi^l$ becomes a simple difference in pressures between blocks $a$ and $b$, where $T_j^l$ is a phase transmissibility. These assumptions are not required by the method, but help to simplify the further description.

*Nonlinear unknowns*

The system of equations (3) is the discretized form of flow and transport equations for general multi-component fluid. Here, we used a Fully Implicit Method (FIM) time approximation. It requires the $(x_{cj}^l \rho_j^l T_j^l \Delta\psi^l)$ flux term to be defined based on nonlinear unknowns at a new timestep $(n+1)$ and introduces nonlinearity to the system of governing equations. Another source of nonlinearities comes from the additional assumption on instantaneous thermodynamic equilibrium, which is required to close the system.

Several different strategies exists for the nonlinear solution of the resulting system, see [1], and [11] for an extensive description and examples. Here, we used the overall molar formulation suggested by Collins et al. [3]. In this formulation, thermodynamic equilibrium is assumed at every nonlinear iteration of solution of Eq. 3. For the control volume at multiphase conditions with $n_p$-phases, the following system of equations needs to be solved:

$$F_c = z_c - \sum_{j=1}^{n_p} \nu_j x_{cj} = 0, \tag{4}$$

$$F_{c+n_c} = f_{c1}(p, T, \boldsymbol{x}_1) - f_{cj}(p, T, \boldsymbol{x}_j) = 0, \tag{5}$$

$$F_{j+n_c \times n_p} = \sum_{c=1}^{n_c} (x_{c1} - x_{cj}) = 0, \tag{6}$$

$$F_{n_p+n_c \times n_p} = \sum_{j=1}^{n_p} \nu_j - 1 = 0. \tag{7}$$

Here $z_c = \sum_j x_{cj}\rho_j s_j / \sum_j \rho_j s_j$ is overall composition and $f_{cj}(p, T, x_{cj})$ is the fugacity of component $c$ in phase $j$. This procedure is called a multiphase flash [24]. For a given overall composition $z_c$, the solution of (4)-(7) provides molar fractions for each component $x_{cj}$ and phase fractions $\nu_j$.

In the overall molar formulation, the unknowns are $p$ and $z_c$. They fully define the physical state $\boldsymbol{\omega}$ for a given control volume. Once multiphase flash is solved, it can provide derivatives of all properties in (3) with respect to nonlinear unknowns using the inverse theorem, see [11] for details.

*General form of governing equations*

We can re-write Eq. 3 as the component of a residual vector in an algebraic form

$$\begin{aligned} r_c(\boldsymbol{\xi}, \boldsymbol{\omega}, \mathbf{u}) &= a(\boldsymbol{\xi}) \left(\alpha_c(\boldsymbol{\omega}) - \alpha_c(\boldsymbol{\omega}_n)\right) \\ &- \sum_l \beta_c^l(\boldsymbol{\omega}) b^l(\boldsymbol{\xi}, \boldsymbol{\omega}) + \theta_c(\boldsymbol{\xi}, \boldsymbol{\omega}, \mathbf{u}) = 0. \end{aligned} \tag{8}$$

Here, we defined

$$\alpha_c(\boldsymbol{\omega}) = (1 + c_r(p - p_{ref})) \sum_j x_{cj} \rho_j s_j, \tag{9}$$

$$a(\boldsymbol{\xi}) = V(\boldsymbol{\xi}) \phi_0(\boldsymbol{\xi}), \tag{10}$$

$$\beta_c(\boldsymbol{\omega}) = \sum_p x_{cj} \frac{k_{rj}}{\mu_j} \rho_j, \tag{11}$$

$$b(\boldsymbol{\xi}, \boldsymbol{\omega}) = \Delta t T^{ab}(\boldsymbol{\xi})(p^b - p^a), \tag{12}$$

$$\theta_c(\boldsymbol{\xi}, \boldsymbol{\omega}, \mathbf{u}) = \Delta t \sum_j \rho_j x_{cj} q_j(\boldsymbol{\xi}, \boldsymbol{\omega}, \mathbf{u}). \tag{13}$$

In addition, $c_r$ is the rock compressibility, $T^{ab}$ is the geometric part of transmissibility (which involves permeability and the geometry of the control volume), $\boldsymbol{\omega}$ and $\boldsymbol{\omega}_n$ are nonlinear unknowns at the current and the previous timestep respectively, and $\mathbf{u}$ is a vector of well control variables.

The operator $\alpha_c$ is dependent on the properties of rock and fluid, and independent of spatially distributed properties (initial porosity) as in the case of the operator $a$. Similarly, the divergence operator is present as a fluid-related operator $\beta_c$ independent of spatial distributed properties (permeability) and the discretization-related operator $b$. The same approach can be applied for the well source/sink operator $\theta_c$, but for simplicity we did not apply it here.

**Linearization methods**

In this section, we describe different types of linearization using the general algebraic form of governing equations (8).

*The standard linearization approach*

To solve nonlinear system (8), we need to linearize it. The conventional approach in reservoir simulation is based on the application of the Newton-Raphson method. In each iteration of this method, we need to solve a linear system of equations of the following form

$$\mathbf{J}(\boldsymbol{\omega}^k)(\boldsymbol{\omega}^{k+1} - \boldsymbol{\omega}^k) = -\mathbf{r}(\boldsymbol{\omega}^k), \tag{14}$$

where $\boldsymbol{J}$ is the Jacobian defined at nonlinear iteration step $k$.

The typical approach requires a sequential assembly of the residual and the Jacobian based on numerical approximations of the analytic relations in (9)-(13). This may demand an interpolation in tables (for standard PVT correlations or relative permeabilities), or a solution of the highly nonlinear equations (for EoS-based properties). Each property evaluation requires a storage space for both values of the property and its derivatives with respect to the nonlinear unknowns.

Most reservoir simulation software performs numerical- [25]or hand-differentiation [9] of each property with respect to nonlinear unknowns. In this work, we utilized the ADGPRS framework [11] for the implementation of conventional and newly proposed linearization procedures.

*Operator-based linearization*

Here, we propose a new strategy for the linearization of the reservoir simulation problem described by Eq. 8. As can be seen from the structure of each operator in (9)-(12), this system is based on a complex combination of different nonlinear properties and relations. Since we fixed our space and time approximation, the discretization error can be controlled only by the variation of the

timestep size $\Delta t$ and the characteristic size of the mesh embedded in the $T^{ab}$ term. Both of these errors are controlled by the operators $\psi$ and $\theta_c$.

The operators $\alpha_c$ and $\beta_c$ represent the physics-based terms. The accuracy of the nonlinear physics representation is controlled by these two operators (and a part of $\theta_c$). In conventional simulation, we introduce all the nonlinear properties into the conservation equation as is. Next, the nonlinear solver tries to resolve all the details of the nonlinear description, struggling sometimes with unimportant features due to the numerical nature of the property representations.

The Operator-Based Linearization (OBL) strategy, proposed in this work, is based on the simplified representation of the nonlinear operators $\alpha_c$ and $\beta_c$ in the parameter-space of a simulation problem. For simplicity, let us assume in the following derivations and implementation that the system of equations (8) describes flow and transport in a binary system. In this case, we only have two independent variables in the overall molar formulation - pressure $p$ and one independent overall composition $z$ (the second is dependent based on the constraint $z_1 + z_2 = 1$). For an isothermal reservoir simulation, the range in the parameter space for pressure is fully defined by the injection/production conditions on wells. The range of $z$ is obviously restrained by $[0, 1]$.

In the further numerical examples, we uniformly discretize the parameter space with a fixed number of points $N$. The interpolation intervals are defined as $[P_1, P_2, \ldots, P_N]$ and $[Z_1, Z_2, \ldots, Z_N]$. Next for $p \in [P_i, P_{i+1}]$ and $z \in [Z_j, Z_{j+1}]$ we define

$$p_i = \frac{p - P_i}{P_{i+1} - P_i},\ z_j = \frac{z - Z_j}{Z_{j+1} - Z_j}, \tag{15}$$

and the auxiliary relation $f_{i,j} = f(P_i, Z_j)$. Based on $p_i$, $z_j$ and $f_{i,j}$, the interpolant of function $F_f$ can be defined as

$$F_f(p, z) = (1 - z_j)[(1 - p_i)f_{i,j} + p_i f_{i+1,j}] + z_j[(1 - p_i)f_{i,j+1} + p_i f_{i+1,j+1}], \tag{16}$$

with corresponding gradients

$$\frac{\partial F_f}{\partial p} = \frac{(1-z_j)(f_{i+1,j} - f_{i,j}) + z_j(f_{i+1,j+1} - f_{i,j+1})}{P_{i+1} - P_i}, \tag{17}$$

$$\frac{\partial F_f}{\partial z} = \frac{(1-p_i)(f_{i,j+1} - f_{i,j}) + p_i(f_{i+1,j+1} - f_{i+1,j})}{Z_{j+1} - Z_j}. \tag{18}$$

Similarly to [17], the error between an interpolant and function can be evaluated based on the following relation

$$|f - F_f| \leq \frac{V_{\boldsymbol{\omega}}^2}{4} \sup_{\boldsymbol{\omega}} \left| \frac{\partial^2 f}{\partial \boldsymbol{\omega}^2} \right|, \tag{19}$$

where $V_{\boldsymbol{\omega}} = ||\Delta \boldsymbol{\omega}_m||$.

To evaluate $\hat{\alpha}_c(p,z)$ and $\hat{\beta}_c(p,z)$ in the course of the simulation, we apply an interpolation

$$\hat{\alpha}_c(p,z) = F_{\alpha_c}(p,z), \quad \hat{\beta}_c(p,z) = F_{\beta_c}(p,z). \tag{20}$$

This representation helps to provide a continuous description of the physics-based operators in the proposed approach. In the examples below, the discretization of the entire parameter space of the problem is applied at the pre-processing stage. In Fig. 1, an example of all operators parameterized at $N = 64$ is shown for a binary compositional system described below. For a general purpose simulation, it is possible to apply this approach adaptively, following the idea of a compositional space parametrization [18, 12]. The example of adaptive interpolation applied to the Operator-Based Linearization is described by Khait and Voskov [26].

In the proposed approach, the number of points in the interpolation controls the accuracy of the approximation of the nonlinear physics, similar to the accuracy of the approximation in space and time being controlled by the grid size. The error described by (19) is similar to the truncation error in the discretization of equation (8). The nonlinear solver deals here with a simplified representation directly expressed as a piece-wise linear combination of nonlinear unknowns. Also, the relation (17)-(18) provides direct derivatives with respect to nonlinear unknowns, which significantly simplifies the evaluation and assem-

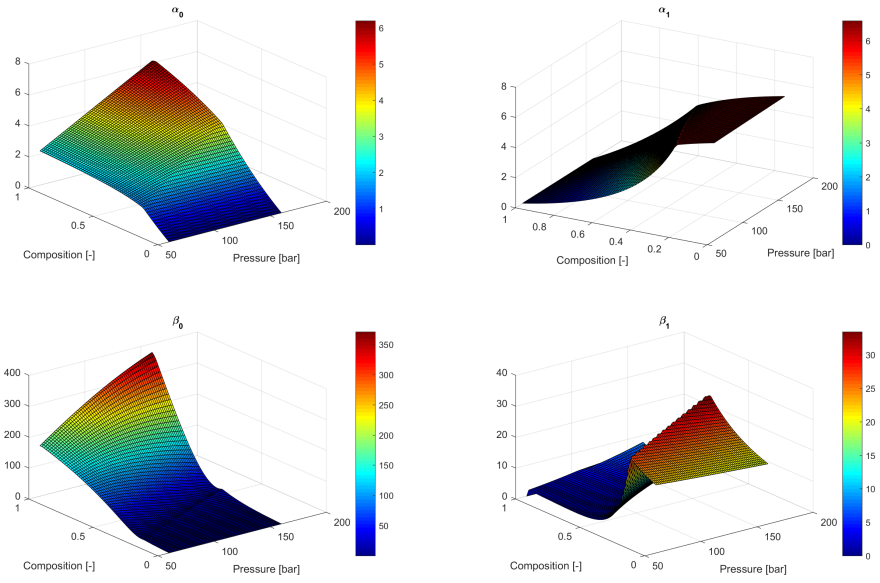


Figure 1: All operators for a binary compositional system parameterized at $N = 64$.

bly of Jacobians. In the next section, we provide several numerical examples to illustrate the proposed approach.

### Solution method

Once each operator in (8) is linearized, the residual vector $\mathbf{r}$ and the Jacobian $\mathbf{J}$ can be assembled. The overall-molar formulation does not require a secondary set of equations [3, 11] and we can apply the linear solver directly to system (14). In this work, we employed GMRES with the two-stage Constrained Pressure Residual (CPR) preconditioner [27] as a linear solver. For details on the linear solution of general-purpose simulation problems, see [8]. Once the linear solution is found, we need to update the nonlinear unknowns. Here we applied a standard Newton-Raphson update with the maximum allowed local change in the overall composition $\Delta z = 0.1$.

An important part of the nonlinear solver is a timestep control. This control may include different types of heuristics to connect timestep size changes in

different variables from the previous timestep [28]. Here, we employ a simple strategy:

- We start with a pre-defined minimal timestep $\Delta t_{min}$;
- if the nonlinear solver converges in a given number of iterations $N_i$, for the current timestep, we multiply the next timestep by a fixed ratio $\gamma$;
- if the nonlinear solver fails to converge, we divide the next timestep by the same constant $\gamma$;
- if the maximum step $\Delta t_{max}$ is reached, we keep it for further simulation;
- finally, if the timestep is cut to the minimal acceptable value ($10^{-8}$ days), the simulation is stopped.

In the examples below, we use a fixed set of parameters, where $\Delta t_{min} = 10^{-3}$ days, $N_i = 30$, $\gamma = 2$ and $\Delta t_{max} = 10$ days. The convergence of the nonlinear solver is based on the following criterion: $max_i|R_i/(\alpha a_i)| < 10^{-5}$, where $i$ is a grid block number.

**Numerical results**

In this section, we compare the numerical results obtained by employing OBL approach against the conventional linearization, used as a reference solution. The comparison covers different physical processes, modeled in 1D and 3D reservoirs.

*One-dimensional homogeneous reservoir*

Here we introduce two types of physical descriptions corresponding to different oil recovery processes: waterflooding (immiscible displacement) and gas injection (miscible displacement). Physical properties for these simulations are described in Appendix A.

A homogeneous 1D reservoir of 1000 m length with one injection and one production well in the first and last grid blocks was modeled first. Constant porosity $\phi_0 = 0.2$ and permeability $k = 100$ mD are used in this model. We

apply a finite-volume discretization on a standard Cartesian grid with block size $\Delta x = 1$, $\Delta y = 10$ and $\Delta z = 10$ m. For the well discretization, the Peaceman formula [29] is used. The injection well is controlled by a water rate $q_w = 20$ $\mathrm{m}^3$/day, and the production well is controlled by a bottom hole pressure $p^w = 100$ bars.

We run a set of simulations and compare the reference solution, based on a conventional linearization method, with results performed at different resolutions of interpolation tables in the OBL approach. For simplicity, we use the equal number of points for each unknown ($p$ and $z$) with uniformly distributed values in the range between $p_{min}$ and $p_{max}$ for pressure, and between 0 and 1 for the composition.

In the immiscible displacement problem, $p_{min} = 50$ and $p_{max} = 650$ were used to cover the parameter space completely. The corresponding average maximum CFL number for this problem is equal to 13.0, which can be interpreted as the ratio between the timestep size of the performed (Fully Implicit) simulation and the timestep restricted by an explicit transport approximation (e.g., in the Implicit Pressure Explicit Saturation (IMPES) method). The total number of timesteps in this simulation is $N_t = 63$.

The results of the first simulation are displayed in Table 1. The number of points used by each unknown for representation of operators $\alpha_c$ and $\beta_c$ is in the first column. The second column indicates the number of nonlinear iterations used in the solution. The third and fourth columns correspond to errors in pressure and composition solution, compared to the reference simulation, that are introduced by the method. The last column shows the CPU time for each simulation.

In Fig. 2, we present a spatial distribution of the water overall molar fraction and pressure by the end of the simulation at time $t = 500$ days. In this figure you can see the difference between the solution with conventional linearization of nonlinear physics vs. the parametrized solutions with four different resolutions of parameter space. The finest resolution shown in the figure contained only 16 points for each unknown. However, it manages to reproduce standard sim-

Table 1: Results of 1D immiscible displacements simulation

| Resolution | Iters. | $E_p$, % | $E_z$, % | CPU, sec |
|---|---|---|---|---|
| Standard | 528 | - | - | 2.0 |
| $64 \times 64$ | 521 | 0.02 | 0.01 | 2.0 |
| $32 \times 32$ | 468 | 0.06 | 0.04 | 1.8 |
| $16 \times 16$ | 422 | 0.27 | 0.19 | 1.6 |
| $8 \times 8$ | 365 | 1.04 | 0.75 | 1.4 |
| $4 \times 4$ | 316 | 6.40 | 3.66 | 1.3 |
| $2 \times 2$ | 146 | 51.23 | 22.68 | 0.8 |

ulation results quite accurately with a smaller number of nonlinear iterations. The simulation time is not significantly different for this simulation since it is relatively short. However, you can see the reduction in simulation time almost proportional to the reduction in the number of nonlinear iterations.

Next, we describe the simulation results for the miscible displacement problem. Unlike in the first case, where all the fluid properties were computed based on a simplified correlation (see Appendix A), in the compositional case, fluid-based properties were computed based on a solution of a highly-nonlinear cubic Equation of State (EoS). Notice that between the injection gas phase and the initial liquid phase conditions, the solution passes through the two-phase region. Here, the derivatives of the phase fractions $x_{cj}$ with respect to nonlinear unknowns are obtained from (4)-(7), which makes the combination of properties even more nonlinear.

The results of the miscible displacement simulation are displayed in Table 2. Similar to the immiscible displacement case, we used the same resolutions for intervals in pressure and composition. However, in the case of gas injection, the interval of pressure changes is lower and $p_{min} = 50$ and $p_{max} = 150$ bars. Well controls were set to a gas rate $q = 2000$ m$^3$/day in the injection well and a pressure $p^w = 70$ bars in the production well. For this case, the corresponding average $\text{CFL}_{max} = 11.5$ and $N_t = 60$ timesteps performed in the simulation.

Table 2 displays the same tendency as in the immiscible displacement case.

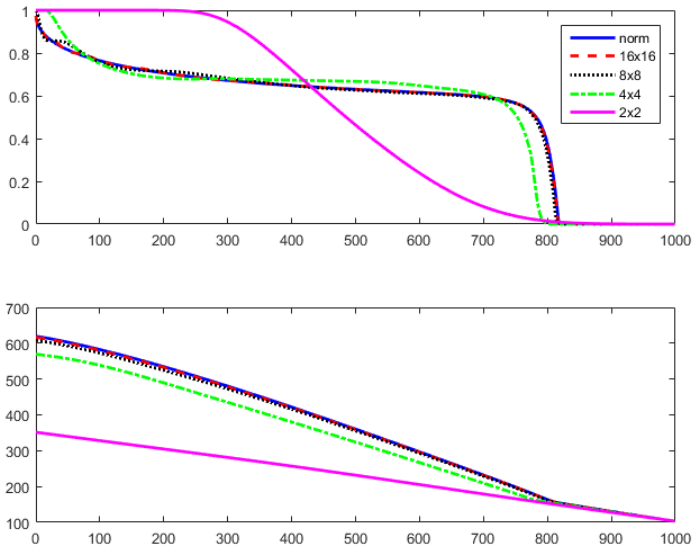


Figure 2: Comparison between overall molar fraction (upper) and pressure (lower) solutions for different resolutions of parametrization in the immiscible displacement test case

With the increasing resolution, the error between the parametrized and the conventional solutions decreases while the number of nonlinear iterations increases. Notice that in this case, the conventional simulation requires significantly larger time than any simulation based on OBL. It can be explained by a more expensive linearization step in the conventional approach which requires multiphase flash and solution of EoS to the evaluate properties and their derivatives in each control volume at every nonlinear iteration. In contrast, the OBL approach requires these calculations only in a limited number of interpolation points at the pre-processing stage. This explains a significant difference in performance between conventional and OBL approaches.

Displacement profiles for both overall molar fraction of the first component ($C_1$) and pressure are shown in Fig. 3 at time $t = 500$ days. Again, the finest resolution shown in the figure with only 16 points is capable of reproducing the conventional simulation results with the reduced number of nonlinear iterations. In Fig. 4, the most nonlinear operator for this system $\boldsymbol{\beta}_2$ is shown for different

Table 2: Results of 1D miscible displacement simulation

| Resolution | Iters. | $E_p$, % | $E_z$, % | CPU, sec |
|---|---|---|---|---|
| Standard | 448 | - | - | 10.8 |
| $64 \times 64$ | 386 | 0.03 | 0.01 | 2.7 |
| $32 \times 32$ | 364 | 0.12 | 0.04 | 1.9 |
| $16 \times 16$ | 343 | 0.65 | 0.16 | 1.6 |
| $8 \times 8$ | 337 | 2.36 | 0.82 | 1.4 |
| $4 \times 4$ | 335 | 3.74 | 3.34 | 1.2 |
| $2 \times 2$ | 145 | 62.24 | 16.39 | 0.8 |

resolutions of the parameterized space $N$ for two limiting pressures $p = 60$ and $p = 160$. A full shape of the operator $\boldsymbol{\beta_2}$ can be seen in Fig. 1. It is clear that at a low resolution of parameterized space ($N = 2$ and $N = 4$), the nonlinearity of the operator is not resolved, which explains a large errors $E_z$ in Table 2. However, starting at $N = 8$, the nonlinearity of the operator reproduced quite accurately, which drops the error $E_z < 1\%$.

*Three-dimensional heterogeneous reservoir*

Here we present the simulation results for a three-dimensional test based on the upper 5 layers of the SPE10 reservoir [30]. Buoyancy is neglected, and the vertical displacement is driven by convective forces only. The injector well was placed in the middle with four production wells in each corner of the model. All wells were perforated into all layers and operated at the same controls as in the previous model. Both porosity and permeability are highly heterogeneous in this case (15 orders of magnitude difference) which explains the very scattered results in Fig 5. The number of timesteps in this simulation $N_t = 113$. Again, we compare the conventional solution with a solution based on an interpolation of operators. It can be seen that the error introduced by all resolutions is mostly located at the displacement interfaces and still provide a reasonable approximation of the reference solution. With a finer resolutions, the difference in the results is almost indistinguishable as can be seen in both the error map of the solution with $8 \times 8$ resolution and cross-section distributions.

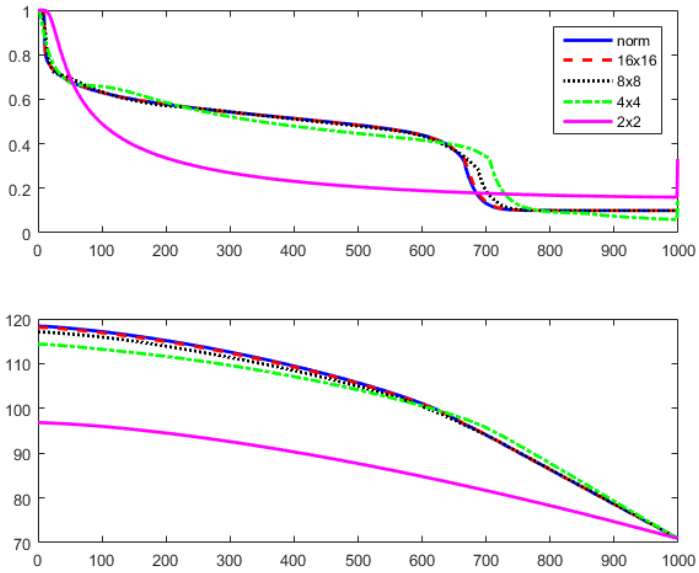


Figure 3: Comparison between overall molar fraction (upper) and pressure (lower) solutions for different resolutions of parametrization in the miscible displacement test case

The performance of the full resolution study is shown in Table 3. The improvement in the number of nonlinear iterations in a highly heterogeneous 3D reservoir model looks similar to 1D homogeneous case. Notice that this type of displacement is characterized by a larger average $\mathrm{CFL}_{max} = 223.1$, which often makes the nonlinear convergence complicated when the physical parameters are fully refined. The improvement in CPU time is also similar and proportional to the number of nonlinear iterations.

Similar observations can be carried out for a 3D miscible displacement case. In this simulation, the average $\mathrm{CFL}_{max} = 167.6$ and the number of timesteps $N_t = 214$. The comparison between the reference solution and the solution, based on interpolated operators, is shown in Fig. 6. Again, the solution based on the coarse interpolation tables still provides a reasonable approximation for the reference solution with an error distributed along the displacement fronts. The full convergence study for this case is shown in Table 4. The improvement in

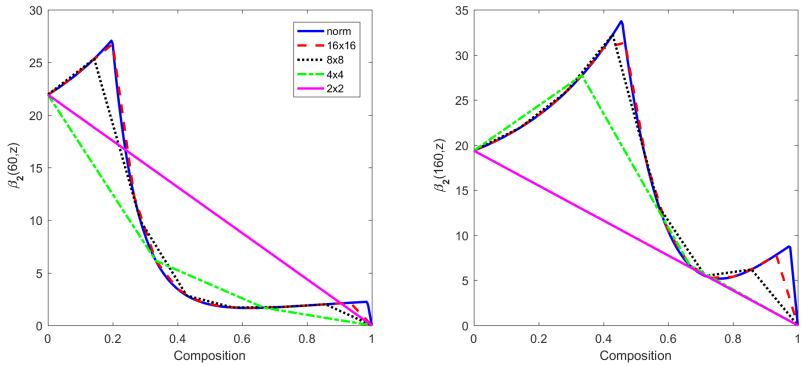


Figure 4: Operator $\boldsymbol{\beta_2}$ for miscible displacement case at end-point pressures and different resolutions in composition

Table 3: Results of 3D immiscible displacement simulation

| Resolution | Iters. | $E_p$, % | $E_z$, % | CPU, sec |
|---|---|---|---|---|
| Standard | 583 | - | - | 651.6 |
| $64 \times 64$ | 577 | 0.03 | 0.01 | 629.5 |
| $32 \times 32$ | 562 | 0.10 | 0.02 | 604.2 |
| $16 \times 16$ | 554 | 0.41 | 0.10 | 593.4 |
| $8 \times 8$ | 529 | 2.54 | 0.47 | 563.4 |
| $4 \times 4$ | 473 | 6.49 | 2.05 | 528.0 |
| $2 \times 2$ | 320 | 101.35 | 13.13 | 362.6 |

simulation time for the OBL approach is still quite significant in comparison to the conventional approach due to the reduction in expensive EoS computations and more efficient assembly of the Jacobian.

The approach proposed here translates all the nonlinear relations into linearized versions. This approximation is directly based on nonlinear unknowns, which significantly improves the behavior of the nonlinear solver. One can balance between the more accurate representation of physics and the performance of the nonlinear solver in the simulation. A significant improvement in simulation time can be achieved due to the reduction in expensive property evaluations in the course of simulation.

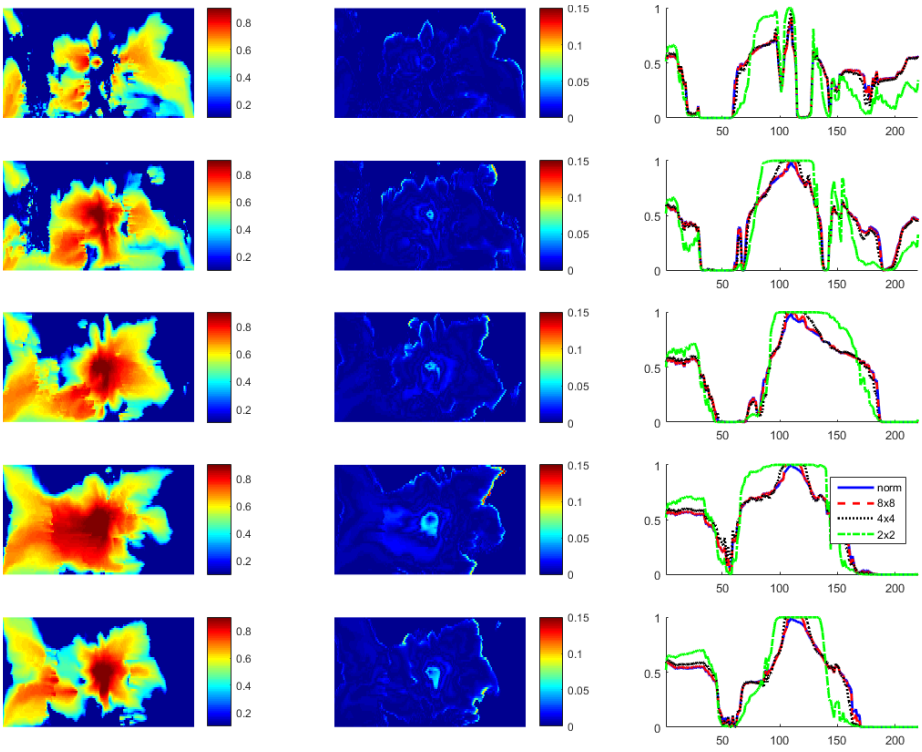


Figure 5: Overall molar fractions: the reference solution based on conventional approach, the error between reference solution and OBL solution with 8x8 interpolation table and cross-section solution at several OBL resolutions for immiscible displacement simulations in reservoir contains 5 upper layers of the SPE10 problem

### Consistency of numerical solution

In this section, we demonstrate the consistency of the proposed linearization method assuming that the original problem described by (1) has a numerical solution. To simplify analysis, we assume that the model is limited by a 1D reservoir with Cauchy boundary conditions on left and right side. This simplifies the spacial discretization, which yields to the following equation in vector form for the block $i$:

$$\begin{aligned} \boldsymbol{r}_i(\boldsymbol{\omega}) &= (\boldsymbol{\alpha}_i(\boldsymbol{\omega}) - \boldsymbol{\alpha}_i(\boldsymbol{\omega}_n)) \\ &- \gamma\left(\boldsymbol{\beta}_i(\boldsymbol{\omega})(p_{i+1} - p_i) - \boldsymbol{\beta}_{i-1}(\boldsymbol{\omega})(p_i - p_{i-1})\right) = 0, \end{aligned} \tag{21}$$

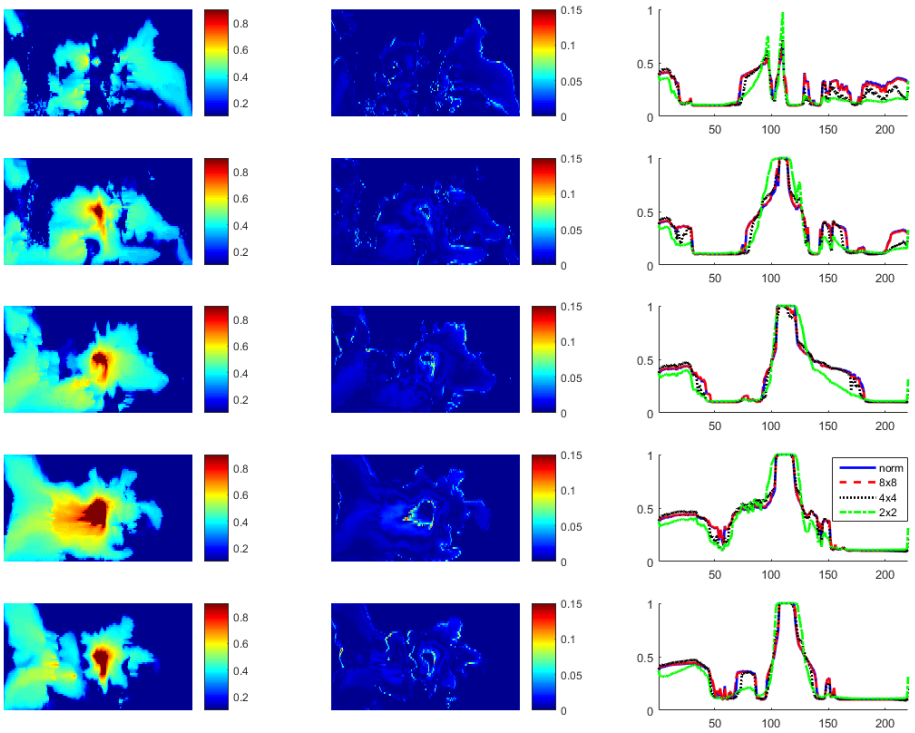


Figure 6: Overall molar fractions: the reference solution based on conventional approach, the error between reference solution and OBL solution with 8x8 interpolation table and cross-section solution at several OBL resolutions for miscible displacement simulations in reservoir contains 5 upper layers of the SPE10 problem

where $\gamma = \Delta t T/(\phi_0 V)$.

The internal Jacobian row of the equation can be written as:

$$J = \begin{bmatrix} \gamma \boldsymbol{B}_{i-1}(p_i - p_{i-1}) - \gamma \boldsymbol{\beta}_{i-1} \times \mathbf{e}_p \\ \boldsymbol{A}_i - \gamma \boldsymbol{B}_i(p_{i+1} - p_i) + \gamma(\boldsymbol{\beta}_i + \boldsymbol{\beta}_{i-1}) \times \mathbf{e}_p \\ -\gamma \boldsymbol{\beta}_i \times \mathbf{e}_p \end{bmatrix}^T \tag{22}$$

where

$$\boldsymbol{A} = \left[\frac{\partial \alpha_i}{\partial \omega_j}\right], \ \boldsymbol{B} = \left[\frac{\partial \beta_i}{\partial \omega_j}\right], \ i, j = 1, \ldots, n_c \tag{23}$$

and $\mathbf{e}_p = [1\ 0\ \ldots\ 0]^T$ is a $n_c$-vector. We can present the Jacobian as a sum of

Table 4: Results of the 3D miscible displacement simulation

| Resolution | Iters. | $E_p$, % | $E_z$, % | CPU, sec |
|---|---|---|---|---|
| Standard | 1025 | - | - | 2074.4 |
| $64 \times 64$ | 951 | 0.06 | 0.01 | 1101.7 |
| $32 \times 32$ | 922 | 0.30 | 0.03 | 1079.2 |
| $16 \times 16$ | 869 | 1.40 | 0.11 | 1015.1 |
| $8 \times 8$ | 807 | 4.28 | 0.47 | 950.1 |
| $4 \times 4$ | 783 | 22.81 | 3.15 | 966.3 |
| $2 \times 2$ | 488 | 70.49 | 6.77 | 612.7 |

two matrix

$$J = J_p + J_z = \begin{bmatrix} -\gamma\boldsymbol{\beta}_{i-1} \times \mathbf{e}_p \\ \gamma(\boldsymbol{\beta}_i + \boldsymbol{\beta}_{i-1}) \times \mathbf{e}_p \\ -\gamma\boldsymbol{\beta}_i \times \mathbf{e}_p \end{bmatrix}^T + \begin{bmatrix} \gamma\boldsymbol{B}_{i-1}(p_i - p_{i-1}) \\ \boldsymbol{A}_i - \gamma\boldsymbol{B}_i(p_{i+1} - p_i) \\ 0 \end{bmatrix}^T \tag{24}$$

where $J_p$ corresponds to the mostly elliptic part of the problem and $J_z$ corresponds to the mostly hyperbolic part. For the consistent solution of the original problem, the matrix $J_p$ expressed in the conventional form of $\boldsymbol{\beta}_i$ should be diagonally dominated. It is clear that the diagonal dominance of $J_p$ will not be affected by the errors in interpolation of $\boldsymbol{\beta}_i$ since these errors will cancel each other in diagonal and off-diagonal part. This conclusion is also valid in a multi-dimensional case.

It is more complicated to perform the analysis of matrix $J_z$ in general case. In the incompressible limit, the error bound defined by (19) will guarantee that the approximation schema is contractive for interpolation operators when the original scheme is contractive which is sufficient for the stability. The eigenvalues of sub-matrices $\hat{\boldsymbol{A}}_i$ and $\hat{\boldsymbol{B}}_i$ related to derivatives of composition will define the hyperbolicity of solution. Notice, that transport in binary systems is always hyperbolic since the only eigenvalue is always real. For systems with a larger number of components, the simulation for a coarse resolution of parameter space with uniform parametrization may fail to converge, as was observed by Khait and Voskov in [26]. This can be explained by the potential loss of hyperbol-

icity in systems with a large number of components. As the solution for this problem, the parametriation can be adjusted to follow tie-lines which describe the phase equilibrium in a system. As demonstrated in [12], the convexity in tie-line parametrization provides a consistent numerical solution for a gas injection problems with multiple components (up to $n_c = 8$) even in the case of an extremely coarse parametrization and a significant compressibility. We leave these aspects for future investigation.

**Conclusion and Discussion**

We presented a new approach for the assembly of the residual and the Jacobian in reservoir simulation. In this approach, the governing equations are transformed into an operator form where each term is presented as a product of two operators. The first type of operators is fully defined by the physical state of the problem and usually corresponds to the most significant nonlinearities. The second operator depends on both spatial and state variables. Next, we parameterize the first type of operators using a uniformly distributed mesh in the parameter space while treating the second type of operators in a conventional manner. By example of two different binary systems, we demonstrated that a simple linear interpolation in the space of state variables ($p$ and $z$) can reproduce the results of the reference system quite accurately even in the case of a coarse interpolation table. The resolution study in physical space for simplified 1D homogeneous and realistic 3D highly heterogeneous models demonstrated a good convergence for the two types of nonlinear physics related to immiscible and miscible displacement processes. The performance of the nonlinear solver demonstrated an improvement due to operation in a linearized physical space.

The proposed approach has several benefits. The first of them is the simplicity of the application. The fully implicit approximation is a very attractive method due to its unconditional stability. However, the complexity of the evaluation and the storage of all the nonlinear properties and their derivatives makes development and further extension of fully implicit code quite challenging. The proposed approach simplifies the residual and the Jacobian assembly

significantly and provides a unique opportunity for the extension of the physical model. The performance of the Jacobian and the residual assembly can be improved and adjusted to the modern computational architectures by using vectorization of the interpolation operator.

Another benefit of the proposed method is related to nonlinear solvers. Most of them in reservoir simulation are based on a version of Newton's method. The interpolation of residual operators as an explicit function of nonlinear unknowns provides an opportunity for better nonlinear strategies. Advanced nonlinear solvers for the proposed formulation can be designed based on a trust-region method in interpolation tables, similar to the approach proposed in [21] for conventional molar formulation. Following this nonlinear strategy, the potential problems introduced by rapid changes of gradients in the coarse tables can be resolved as well. The fact that the physical kernel of a problem has a multi-linear representation based on nonlinear unknowns may also help to achieve a better preconditioning on a linear level similar to Algebraic Multi-Scale methods [31].

The general-purpose application of the introduced method requires dealing with multi-linear interpolation in a highly dimensional space, especially for compositional problems. The adaptive parametrization approach, developed in [12] for representation of compositional properties, can help in the extension of the method for problems with a large number of components. The accuracy of the approach can be controlled by the error estimator and adaptive resolution in parameter space. An example of a simple error estimator applied for a limited case of property interpolation can be found in [17]. The extension to systems with more than two-phases can be performed based on a tie-simplex parametrization approach [32, 33].

In general, reservoir simulation is always based on the approximation of spatial and temporal discretization. In a lot of cases, this approximation has only a first order of accuracy. At the same time, the description of complex nonlinear physics, embedded into a model, is always very precise. The current realization of the approach, described in this paper, can be seen as a compromise between the accuracy of the nonlinear representation of physics and the performance

of the nonlinear solver. Finding the balance among the different coarsening strategies is the target for the future research.

**Acknowledgement**

We would like to acknowledge Rustem Zaydullin for the research ideas that inspired this work and Mark Khait for the code optimization. We also thank the Stanford University Petroleum Research Institute for Reservoir Simulation (SUPRI-B) program for the permission to use ADGPRS in this research.

**References**

[1] K. Aziz, T. Wong, Considerations in the development of multipurpose reservoir simulation models, in: The 1st and 2nd International Forum on Reservoir Simulation, Alpbach, Austria, 1989, pp. 77–208.

[2] G. Acs, S. Doleschall, E. Farkas, General purpose compositional model., Soc. Petrol. Eng. J. 25 (4) (1985) 543–553.

[3] D. Collins, L. Nghiem, Y.-K. Li, J. Grabenstetter, Efficient approach to adaptive-implicit compositional simulation with an equation of state, Soc. Petrol. Eng. J. 7 (2) (1992) 259–264.

[4] K. Coats, An equation of state compositional model, Soc. Petrol. Eng. J. 20 (1980) 363–376.

[5] A. Abadpour, M. Panfilov, Asymptotic decomposed model of two-phase compositional flow in porous media: Analytical front tracking method for riemann problem, Transport Porous Med. 82 (3) (2009) 547–565. doi:10.1007/s11242-009-9428-8.

[6] A. Lauser, C. Hager, R. Helmig, B. Wohlmuth, A new approach for phase transitions in miscible multi-phase flow in porous media, Adv. in Water Resour. 34 (8) (2011) 957 – 966. doi:http://dx.doi.org/10.1016/j.advwatres.2011.04.021.

[7] D. Voskov, An extended natural variable formulation for compositional simulation based on tie-line parameterization, Transport Porous Med. 92 (3) (2012) 541–557. doi:10.1007/s11242-011-9919-2.

[8] H. Cao, Development of Techniques for General Purpose Simulators, PhD Thesis, Stanford University, 2002.

[9] Geoquest, Eclipse Technical Description 2005A, Schlumberger, 2005.

[10] R. Younis, Modern advances in software and solution algorithms for reservoir simulation, PhD Thesis, Stanford University, 2011.

[11] D. V. Voskov, H. A. Tchelepi, Comparison of nonlinear formulations for two-phase multi-component eos based simulation, J. Petrol. Sci. Eng. 82-83 (2012) 101–111.

[12] R. Zaydullin, D. Voskov, H. Tchelepi, Nonlinear formulation based on an equation-of-state free method for compositional flow simulation, Soc. Petrol. Eng. J. 18 (2) (2013) 264–273.

[13] Y. Zhou, H. Tchelepi, B. Mallison, Automatic differentiation framework for compositional simulation on unstructured grids with multi-point discretization schemes, in: SPE Reservoir Simulation Symposium 2011, Vol. 1, 2011, pp. 607–624.

[14] R. Zaydullin, D. Voskov, S. James, A. Lucia, Fully compositional and thermal reservoir simulation, Comput. Chem. Eng. 63 (2014) 51 – 65. doi:10.1016/j.compchemeng.2013.12.008.

[15] T. Garipov, M. Karimi-Fard, H. Tchelepi, Discrete fracture model for coupled flow and geomechanics, Computational Geosciences 20 (1) (2016) 149–160. doi:10.1007/s10596-015-9554-z.

[16] O. Volkov, D. Voskov, Effect of time stepping strategy on adjoint-based production optimization, Computat. Geosci. 20 (3) (2016) 707–722. doi:10.1007/s10596-015-9528-1.

[17] R. Zaydullin, D. Voskov, H. Tchelepi, Formulation and solution of compositional displacements in tie-simplex space, in: SPE Reservoir Simulation Symposium 2013, Vol. 2, 2013, pp. 1268–1282. doi:doi:10.2118/163668-MS.

[18] D. Voskov, H. Tchelepi, Compositional space parametrization for miscible displacement simulation, TIPM 75 (1) (2008) 111–128. doi:10.1007/s11242-008-9212-1.

[19] Y. Wu, C. Kowitz, S. Sun, A. Salama, Speeding up the flash calculations in two-phase compositional flow simulations the application of sparse grids, J. Comput. Phys. 285 (2015) 88 – 99. doi:http://dx.doi.org/10.1016/j.jcp.2015.01.012.

[20] P. Jenny, H. A. Tchelepi, S. H. Lee, Unconditionally convergent nonlinear solver for hyperbolic conservation laws with s-shaped flux functions, J. Comput. Phys. 228 (20) (2009) 7497 – 7512. doi:http://dx.doi.org/10.1016/j.jcp.2009.06.032.

[21] D. V. Voskov, H. A. Tchelepi, Compositional nonlinear solver based on trust regions of the flux function along key tie-lines, in: SPE Reservoir Simulation Symposium, SPE 141743, 2011. doi:doi:10.2118/141743-MS.

[22] X. Wang, H. Tchelepi, Trust-region based solver for nonlinear transport in heterogeneous porous media, J. Comput. Phys. 253 (2013) 114–137. doi:10.1016/j.jcp.2013.06.041.

[23] B. Li, H. Tchelepi, Nonlinear analysis of multiphase transport in porous media in the presence of viscous, buoyancy, and capillary forces, J. Comput. Phys. 297 (2015) 104–131. doi:10.1016/j.jcp.2015.04.057.

[24] M. Michelsen, The isothermal flash problem: Part ii. phase-split calculation, Fluid Phase Equilibr. 9 (1982) 21–40.

[25] K. Pruess, S. Finsterle, G. Moridis, C. Oldenburg, Y.-S. Wu, General-purpose reservoir simulators: The tough2 family, Bulletin. Geothermal Resources Council 26 (2) (1997) 53–57.

[26] M. Khait, D. Voskov, Operator-based linearization for non-isothermal multiphase compositional flow in porous media, in: ECMOR XIV-15th European Conference on the Mathematics of Oil Recovery, 2016, pp. 1–15.

[27] J. Wallis, R. Kendall, T. Little, Constrained residual acceleration of conjugate residual methods, Soc Pet Eng AIME J (1985) 415–428.

[28] K. Aziz, T. Settari, Petroleum Reservoir Simulation, Applied Science Publishers, 1979.

[29] D. Peaceman, Interpretation of well-block pressures in numerical reservoir simulation., Soc Pet Eng AIME J 18 (3) (1978) 183–194.

[30] M. Christie, M. Blunt, Tenth spe comparative solution project: A comparison of upscaling techniques, SPE Reservoir Eval. & Eng. 4 (4) (2001) 308–316.

[31] Y. Wang, H. Hajibeygi, H. A. Tchelepi, Algebraic multiscale solver for flow in heterogeneous porous media, J. Comput. Phys. 259 (2014) 284 – 303. doi:10.1016/j.jcp.2013.11.024.

[32] A. Iranshahr, D. Voskov, H. Tchelepi, Gibbs energy analysis: Compositional tie-simplex space, Fluid Phase Equilibr. 321 (2012) 49–58. doi:10.1016/j.fluid.2012.02.001.

[33] A. Iranshahr, D. Voskov, H. Tchelepi, Tie-simplex based compositional space parameterization: Continuity and generalization to multiphase systems, AIChE J 59 (5) (2013) 1684–1701. doi:10.1002/aic.13919.

[34] D. Peng, D. Robinson, A new two-constant equation of state, Ind. Eng. Chem. Fundam. 15 (1976) 59–64.

[35] J. Lohrenz, B. Bray, C. Clark, Calculating viscosities of reservoir fluids from their compositions, Soc. Petrol. Eng. J. (1964) 1171–1176doi:10.2118/915-PA.

## Appendix A. Fluid and rock properties

The parameters defined in Table A1 are common for all the models. In this table index $p$ means water in the immiscible displacement model and gas in the miscible displacement model. The Corey-type relative permeabilities are

Table A1: Rock-fluid parameters

| Parameter | Value | Description |
|---|---|---|
| $c_r$ | $10^{-5}$ 1/bar | rock compressibility |
| $S_{pr}$ | 0 | phase residual saturation |
| $S_{or}$ | 0 | oil residual saturation |
| $n_p$ | 2 | phase exponents |
| $n_o$ | 3 | oil exponents |

defined as

$$S_{pe} = (S_p - S_{pr})/(1 - S_{pr} - S_{or}), \tag{A1}$$

$$k_{rp} = (S_{pe})^{n_p}, \quad k_{ro} = (1 - S_{pe})^{n_o}. \tag{A2}$$

The parameters of correlations used for properties in the immiscible displacement example are defined in Table A2. Here we use standard correlations

Table A2: Immiscible displacement parameters

| Param. | Oil | Water | Description |
|---|---|---|---|
| $\rho_p^0$ | 850 kg/m$^3$ | 1000 kg/m$^3$ | surface density |
| $c_p$ | $10^{-4}$ 1/bar | $10^{-5}$ 1/bar | compressibility |
| $\mu_p^0$ | 0.8 cP | 1 cP | viscosity |
| $\beta_p$ | 3.2 $10^{-3}$ 1/bar | 0 | viscosibility |

for density and viscosity of dead-oil:

$$R_\rho = c_p(p - p_{ref}), \quad \rho_p = \rho_p^0(1 + R_\rho + R_\rho^2/2), \tag{A3}$$

$$R_\mu = \beta(p - p_{ref}), \quad \mu_p = \mu_p^0(1 + R_\mu + R_\mu^2/2). \tag{A4}$$

The component mole fractions for this model are defined as $x_{oo} = x_{ww} = 1$ and $x_{ow} = x_{ow} = 0$. Initial saturation $S_{ini} = 0$ and pressure $p_{ini} = 200$ bars were

applied for the initialization of the models.

The next table defines the main parameters for the compositional model describing the gas injection case. In this model, Peng and Robinson [34] Equation

Table A3: Miscible displacement parameters

| C. | $T_c\,K$ | $P_c\,bar$ | $\omega$ | $M_w\,g/mol$ | $k_{i,C_1}$ |
|---|---|---|---|---|---|
| $C_1$ | 190.6 | 46.04 | 0.013 | 16.04 | - |
| $C_8$ | 575.0 | 28.79 | 0.312 | 107.0 | 0.037 |

of State was used to compute density $\rho_p$. For phase viscosity, the LBC correlation [35] was applied. Phase fractions were defined based on a flash calculation [24]. For the initialization of the compositional model, the initial composition $z_{ini} = \{0.1, 0.9\}$ and pressure $p_{ini} = 100$ bars was used.